

Processing of microcellular SiC foams

Part I *Curing kinetics of polycarbosilane in air*

T. J. FITZGERALD, A. MORTENSEN

Department of Materials Science and Engineering, Room 8-401, Massachusetts Institute of Technology, Cambridge, Massachusetts, 02139, USA

Curing kinetics of commercial polycarbosilane have been measured using differential scanning calorimetry in air between 140 and 220 °C. It was found that the total heat of curing increases linearly with temperature. At constant temperature, the rate of heat release can be described by the sum of a first-order kinetic term, and a transient term of much higher order, both depending on the fraction of remaining reaction enthalpy. Constants for both terms increase according to the Arrhenius law, with roughly the same activation energy of about 1.2 kJ mol⁻¹. The heat released in an additional non-isothermal experiment is well described by integration of the isothermal heat-release equations, suggesting that the rate of reaction can be described solely in terms of the fraction transformed and temperature.

1. Introduction

Several ceramics, including nitrides and carbides, can be produced by controlled pyrolysis of polymer precursors. This processing route features low process temperatures, and produces ceramic bodies having shapes easily generated in viscoplastic deformation processes typical of thermoplastic polymers [1–3]. A prominent example is that of fine Si–C and Si–C–Ti–O fibres, which are now produced commercially by controlled pyrolysis of spun preceramic polymer fibres [5, 6].

One of the chief limitations of this ceramic processing method is the shrinkage experienced during conversion of the polymer to the ceramic. This shrinkage results from the escape of various elements from the polymer in the form of low molecular weight gases. During pyrolysis, these elements diffuse through the converting polymer to a free surface, from where they evaporate in the form of molecules such as H₂, CH₄ or CO [5, 7, 8]. The need for these atoms to escape via solid-state diffusion limits ceramics produced by this method to sizes of the order of tens of micrometres if the resulting material is to be pore free [1].

This limitation is circumvented if the polymer-derived ceramics are used to produce the reinforcing phase of a large composite material. In the form of a fine reinforcing phase, conversion of the polymer to a ceramic can take place with easy escape of volatile species, after which the resulting material is used to fabricate a large and fully dense composite material. For this reason, polymer-derived SiC has been largely produced and commercialized in the form of fine reinforcing fibres, such as the NicalonTM fibres produced by Nippon Carbon in Japan.

The present work explored the production of a different type of ceramic reinforcement made using preceramic polymers, namely that of a three-dimensionally interconnected network of struts, otherwise

known as an open-celled foam. In an open-celled foam, all pores of the ceramic can be infiltrated with another phase, e.g. a metal or a ceramic, to produce a fully dense composite material. The resulting composite is composed of two phases which are three-dimensionally interconnected throughout the material, as opposed to usual composites in which the reinforcement takes the form of isolated fibres, whiskers or particles. This type of material has attracted some attention recently, under the name interpenetrating phase composites, largely as a result of the development of novel composite processing techniques [9].

Because open-celled foams are generally produced with thermoplastic polymers, the preceramic polymer processing route is particularly attractive for the production of such ceramic reinforcements. Specifically, we used polycarbosilane to produce open-celled SiC foams using a replication technique, in which the polymer is first infiltrated in the pores left between partially sintered salt preforms. The salt is then leached away with water, and the polycarbosilane foam is converted to SiC by pyrolysis. Although somewhat slow, this process has the advantage of allowing extensive control of reinforcement architecture, allowing in particular the production of very fine and uniform SiC foams.

Polycarbosilane objects are typically cured prior to pyrolysis to transform the polymer from a thermoplastic to a thermoset: cross-linking is critical for objects which must support their own weight, such as fibres and foams, because these would otherwise melt during pyrolysis. The simplest and most commonly used method for curing polycarbosilane is direct oxidation of the polymer by heating in either air or oxygen to around 100–200 °C, which produces cross-linking of side groups on polycarbosilane molecules [10–16]. Using differential scanning calorimetry

(DSC) several researchers have investigated the curing kinetics of polycarbosilane both in air and oxygen. Published DSC curves show that the curing kinetics vary strongly with the nature of the polycarbosilane; however, sharp positive peaks are generally found, showing that polycarbosilane curing is an exothermic process, the rate of which increases rapidly with increasing temperature [5, 10, 12, 13, 17–19].

Most polycarbosilane curing DSC curves found in the literature feature high dynamic scan rates (typically $5^{\circ}\text{C min}^{-1}$ or more), and have relatively poor resolution. In the only published detailed study we found on the curing kinetics of polycarbosilane [18, 19], a few milligrams of commercially available polycarbosilane were placed in a DSC under a neutral nitrogen atmosphere. The polycarbosilane was then quickly heated to elevated temperature. Once the system reached a steady thermal state, the atmosphere was quickly switched over to pure oxygen. The change in atmosphere was reported to be complete within a matter of seconds, thereby providing a near-instantaneous start for the curing reactions. In this way, curing exotherms under isothermal conditions were recorded. The resulting data were fitted to the equation

$$\frac{d\alpha}{dt} = (k_1 + k_2 \alpha^m)(1 - \alpha)^n \quad (1)$$

where α is the fractional conversion, t is time, and k_1 and k_2 are rate constants having an Arrhenius-type dependence on temperature. This equation predicts a maximum in the rate of conversion at some non-zero time.

It will be shown in Part II [20] that the heat released in oxidative curing of polycarbosilane is the most critical factor in the processing of large three-dimensional SiC bodies from this polymer: depending on heat transfer from the body to its surroundings, the exothermic nature of curing may cause internal cracking or melting of the body. A study of the curing kinetics of commercially available polycarbosilane in air was therefore conducted, using differential scanning calorimetry to derive empirical kinetic equations. This work is reported here, and its results have been used in Part II in a computer model of heat transfer during the curing of three-dimensional polycarbosilane foams.

2. Experimental procedure

Commercially available polycarbosilane was used, produced by Nippon Carbon in Japan, and distributed in the United States by Dow Corning (product number X9-6348). Based upon investigations using cryoscopy, Fourier transform-infrared spectroscopy (FT-IR) and $^1\text{H-NMR}$, the structure of commercially available polycarbosilane appears very similar to that of PC-470 [17, 21]: the number average molecular weight is similar, and the molecular weight of commercial polycarbosilane was measured by Spotz to be 1580 ± 80 , which is close to that of PC-470, namely 1550 [21].

Experiments were conducted with a Perkin–Elmer (Norwalk, CT) DSC-7 differential scanning calorimeter. The temperature precision and the temperature accuracy of the DSC-7 are reported to be $\pm 0.1^{\circ}\text{C}$. The calorimetric precision is better than $\pm 0.1\%$. The system was calibrated using indium. The gas flow to the DSC was supplied by a cylinder with an outlet pressure maintained constant throughout the experiment, at the recommended level of 2.1×10^5 Pa.

Polycarbosilane was ground using a mortar and pestle and subsequently sieved. The resulting powder consisted of particles 45–75 μm in diameter. Approximately 2–3 mg powder were weighed using a microbalance of $\pm 1 \mu\text{g}$ accuracy, and placed in a shallow aluminium DSC pan. Following a procedure recommended by Perkin–Elmer, the aluminium pan was left unsealed and placed directly into the sample holder of the DSC. Perforated platinum covers were placed over the sample and reference holders.

Six curing runs were performed under isothermal conditions shown in Table I using the standard “isothermal” software of the DSC-7. Samples were brought up to temperature at the rate of $200^{\circ}\text{C min}^{-1}$ in flowing air, which provided a near instantaneous start to the curing cycle (which typically lasted 12 h). Once the isothermal temperature was reached, data acquisition was begun.

Two additional DSC runs were performed on a single sample of polycarbosilane. During the first run the sample was partially cured under non-isothermal conditions. During the second run, the sample was cured to completion under isothermal conditions. The first run, referred to as run 7, consisted of a dynamic temperature scan performed using the standard “multitasking” software on the DSC-7. In this run, the temperature was raised from 25°C to 220°C at $3^{\circ}\text{C min}^{-1}$, and data were continually collected by microcomputer. Upon reaching 220°C the sample was quickly cooled to 25°C at $200^{\circ}\text{C min}^{-1}$, thereby quenching the reaction. Following this run, the partially cured sample was left undisturbed in the DSC and the system was allowed to come to equilibrium.

The second run, referred to as run 8, was performed on the same sample using the standard “isothermal” software on the DSC-7. The temperature was ramped from 25 – 220°C at $200^{\circ}\text{C min}^{-1}$, thereby providing a near instantaneous start for the isothermal cure cycle. The temperature was held at 220°C for 5 h, during which time the reaction went to completion.

TABLE I Summary of isothermal DSC experiments

DSC run	Temperature ($^{\circ}\text{C}$)	Atmosphere	Duration of DSC run (h)
1	140	Air	12
2	160	Air	12
3	180	Air	12
4	200	Air	12
5	200	Oxygen	5
6	220	Air	6

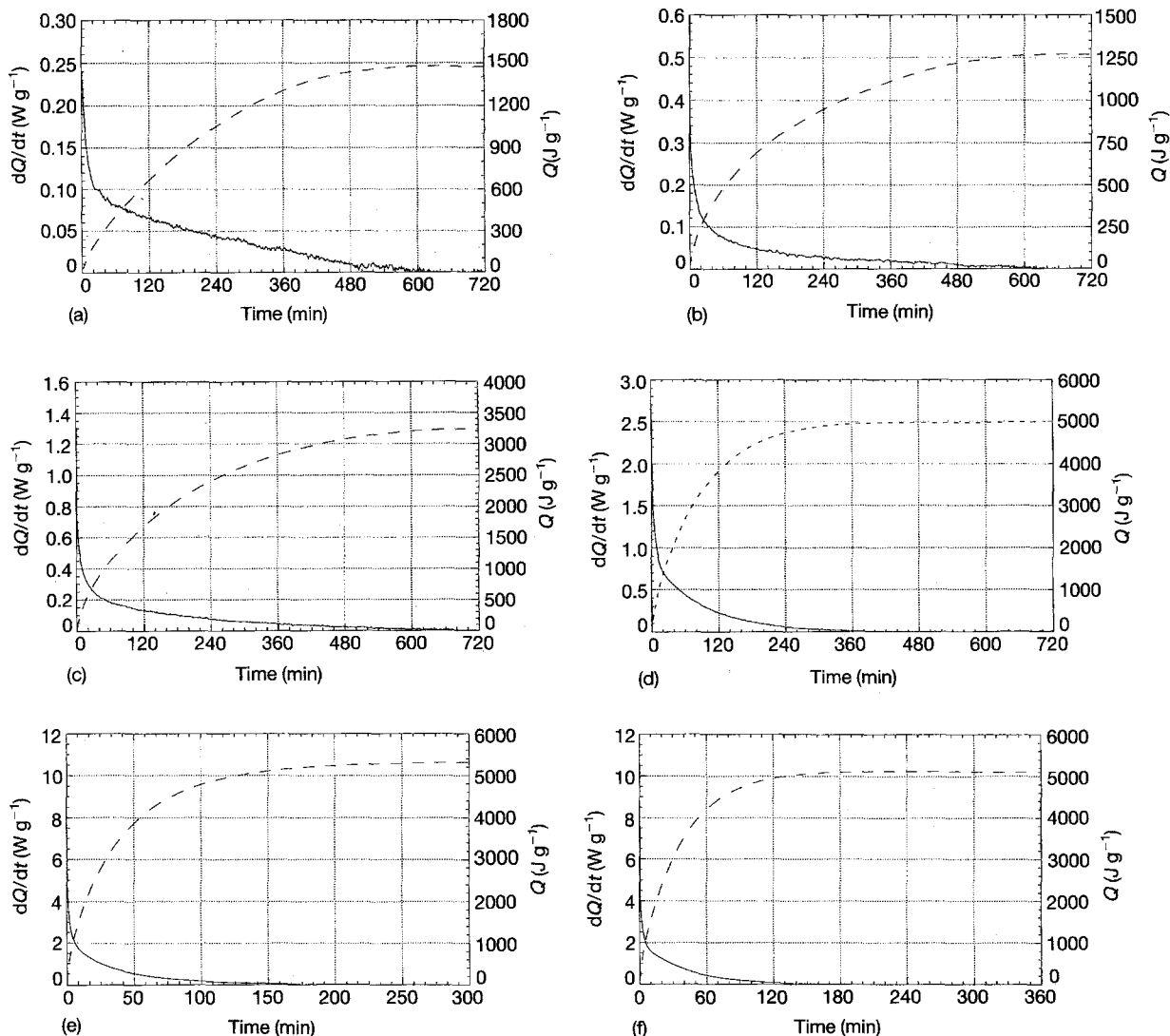


Figure 1 (—) Heat flow and (---) integrated heat of curing as a function of time, for isothermal DSC experiments listed in Table I: (a) run 1, (b) run 2, (c) run 3, (d) run 4, (e) run 5, and (f) run 6.

3. Results

In isothermal DSC experiments, the thermal power supplied by the DSC to the sample to maintain it at the specified temperature was found to increase with time, reaching a plateau after a certain time. The data thus indicate that an exothermic reaction takes place in the samples, which subsides as time progresses. The difference between the constant thermal power supplied by the DSC to the sample when the reaction subsides at greater time (which is system-dependent and varies from run to run) and the power supplied by the DSC to the sample at time t , is therefore the rate of heat generation within the sample due to the reaction at that time. The resulting time-dependent rate of heat generation dQ/dt due to the curing reaction per unit mass of polycarbosilane measured in runs 1–6 is plotted in Fig. 1a–f, respectively.

The rate of heat generation measured with the DSC in run 7 (in which the temperature was ramped), is plotted in Fig. 2a. The DSC curve slopes upward with temperature indicating an exothermic reaction which becomes increasingly pronounced at higher temperatures. The minimum of the curve, which corresponds to the very small rate of polycarbosilane reaction

observed at low temperature, was taken as the reference point to compute the thermal power measured in this run. The heat generated by subsequent isothermal curing of this sample (run 8), was computed as with other isothermal runs, and is given in Fig. 2b.

4. Discussion

The data from runs 1–6 were numerically integrated with respect to time to calculate the cumulative heat of curing as a function of time, drawn as dashed lines in Fig. 1. The value at which the integrated curve levels off corresponds to the total heat of curing at that particular temperature, $Q_{\text{tot}}(T)$, given in Table II and plotted in Fig. 3. As seen in Fig. 3, the total heat of curing can be fitted to the straight line

$$Q_{\text{tot}} = 54.5 T(^{\circ}\text{C}) - 6580 (\text{J g}^{-1}) \quad (T > 121^{\circ}\text{C}) \quad (2)$$

Extrapolating backwards, the reaction appears to begin at 121 °C. The observed linearity of Q_{tot} with

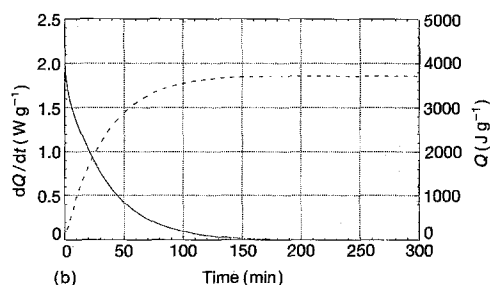
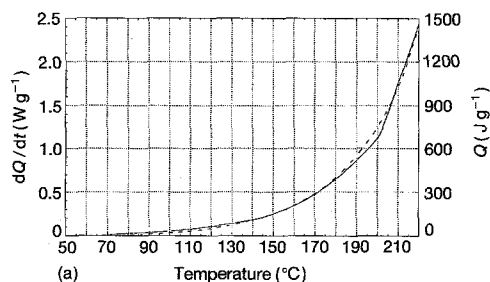


Figure 2 Heat flow and integrated heat of curing for non-isothermal DSC experiments: (a) run 7, scan rate = $3^{\circ}\text{C min}^{-1}$; (b) run 8, partially cured polycarbosilane.

TABLE II Total heat of curing at various temperatures

DSC run	Temperature ($^{\circ}\text{C}$)	Atmosphere	Q_{tot} (J g^{-1})
1	140	Air	(1533)
2	160	Air	(1270)
3	180	Air	3239
4	200	Air	5039
5	200	Oxygen	5312
6	220	Air	5100

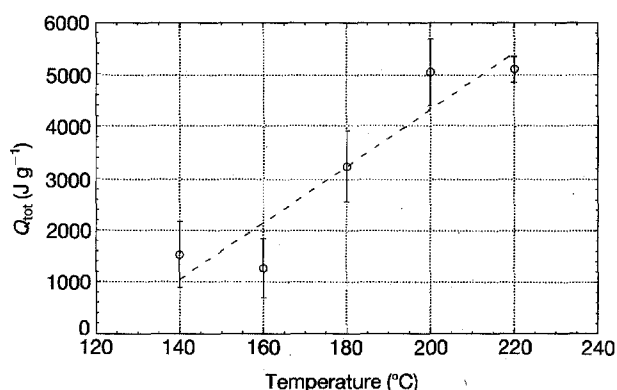


Figure 3 Total heat of curing in air as a function of temperature, DSC runs 1, 2, 3, 4 and 6.

temperature is in agreement with the findings of Taki *et al.* [14, 15] (assuming that their samples were completely cured at reported temperatures): in curing of polycarbosilane, the quantity of oxygen incorporated, and the number of main bond changes of each kind,

were all approximately linear functions of curing temperature. Equation 2 also agrees with data of Ichikawa *et al.* [13] who found that above 180°C , the amount of oxygen incorporated in "PC-470" polycarbosilane increases linearly with the final temperature of a non-isothermal curing cycle in which temperature was raised at $10^{\circ}\text{C h}^{-1}$ (these authors found a transition in the mechanism of oxidation around 180°C , which resulted in a somewhat reduced rate of increase in oxygen incorporation with temperature below 180°C).

It is noted that error bars which have been added to Fig. 3 correspond to the observed system drift for run 4 (observed after the reaction subsided). Data from DSC runs 1 and 2 are not considered entirely reliable, because the DSC curve did not completely level off within the time-frame of the experiment. The results from the numerical integration of the data from these runs are therefore given in parentheses in Table II, as these only provide an estimate of the heat of curing at these temperatures. These data are not used in the data analysis which follows.

For DSC runs 3–6, the heat flow, dQ/dt , and cumulative heat flow, $Q(t)$, were divided by the total heat of curing, $Q_{\text{tot}}(T)$ to calculate $\alpha = Q/Q_{\text{tot}}$, the fraction converted at temperature T . Plots of $d\alpha/dt$ versus $(1 - \alpha)$ are given in Fig. 4a–d. As seen in the curves, at values of $(1 - \alpha)$ below about 0.7, the data obey the equation

$$\frac{d\alpha}{dt} = k_1(1 - \alpha) \quad (3)$$

where k_1 is a rate constant, indicating first-order reaction kinetics. The curve fit is drawn with a dashed line in the figures, from which a value of k_1 was derived. When $k_1(1 - \alpha)$ is subtracted from $d\alpha/dt$ and plotted versus $1 - \alpha$, Fig. 5a–d, the result can be fitted to an equation of the form

$$\frac{d\alpha}{dt} - k_1(1 - \alpha) = k_2(1 - \alpha)^n \quad (4)$$

where k_2 is a rate constant, and n is a dimensionless term. Rewriting Equation 4 gives the overall kinetic expression

$$\frac{d\alpha}{dt} = k_1(1 - \alpha) + k_2(1 - \alpha)^n \quad (5)$$

where k_1 , k_2 and n are constants. The values of k_1 , k_2 , and n for each run are given in Table III.

The rate constants k_1 and k_2 increase with temperature and display a classical Arrhenius-type dependence on temperature, as seen in Fig. 6. The best fit for rate constants k_1 and k_2 is given by

$$k_1 = 6.97 \times 10^6 \exp[-9560/T(\text{K})] \quad (\text{min}^{-1}) \quad (6)$$

$$k_2 = 36.1 \times 10^6 \exp[-9970/T(\text{K})] \quad (\text{min}^{-1}) \quad (7)$$

As shown in Fig. 7, the constant n can be considered a linear function of temperature

$$n = 0.140 \times T(^{\circ}\text{C}) - 15.3 \quad (8)$$

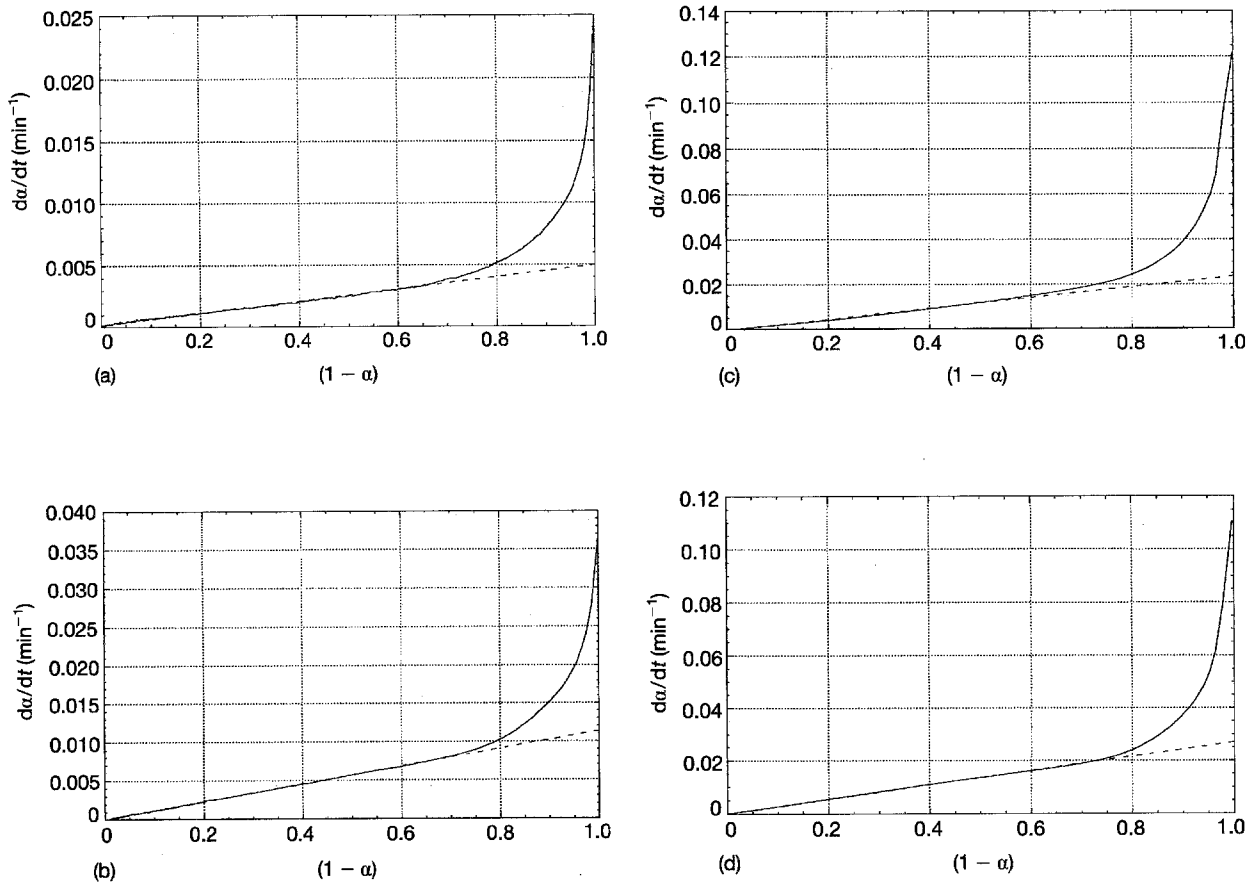


Figure 4 (—) Rate of conversion ($d\alpha/dt$) versus $(1 - \alpha)$ for DSC runs (a) 3, (b) 4, (c) 5, and (d) 6. (---) curve fit.

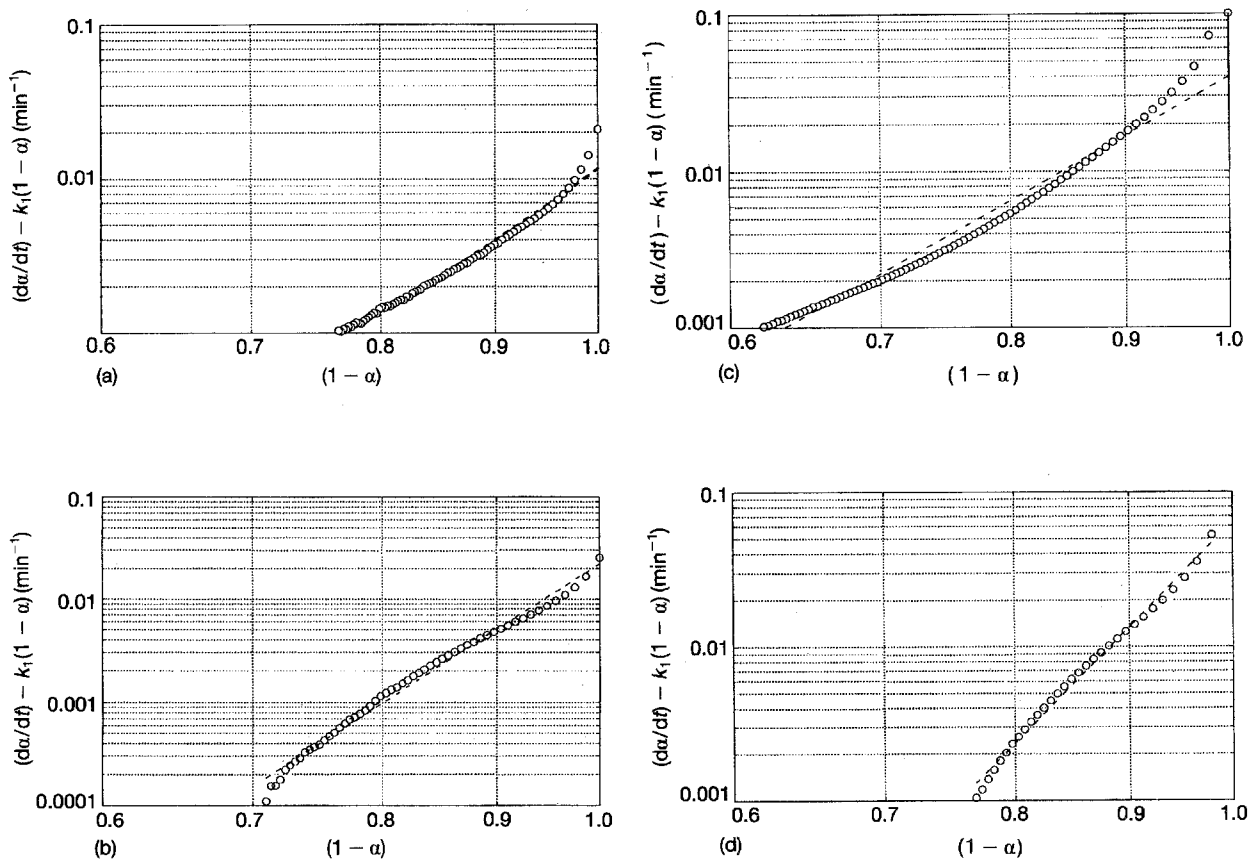


Figure 5 $(\frac{d\alpha}{dt}) - k_1(1 - \alpha)$ versus $(1 - \alpha)$ for DSC runs (a) 3, (b) 4, (c) 5, and (d) 6.

TABLE III Kinetic parameters at various temperatures

Temperature (°C)	Atmosphere	k_1 (10^3 min^{-1})	k_2 (10^2 min^{-1})	n
180	Air	4.86	1.07	9.23
200	Air	11.39	2.21	15.14
200	Oxygen	24.02	3.97	8.09
220	Air	26.97	6.47	14.83

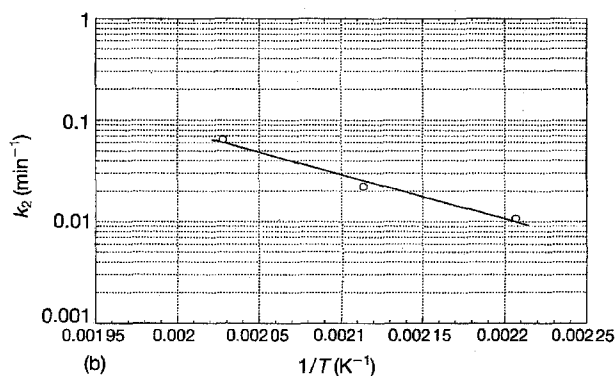
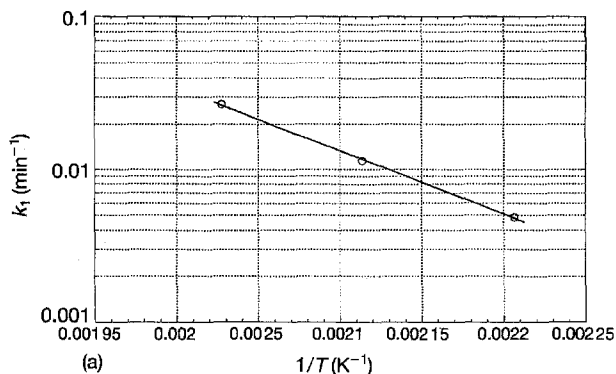


Figure 6 Rate constants as a function of temperature: (a) k_1 , (b) k_2 .

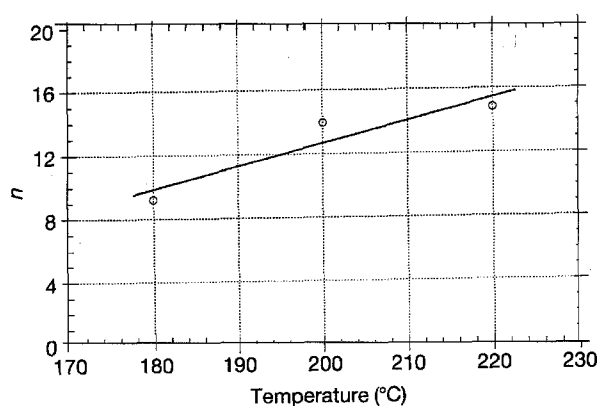


Figure 7 The exponential factor n as a function of temperature.

As shown in Table III, an oxygen-curing atmosphere increases somewhat the rate constants and reduces the exponential term n . The total heat of curing at 200 °C is essentially the same regardless of whether curing is performed in air or oxygen, Table II.

The first-order dependence of reaction rate on $(1 - \alpha)$ at long times (Equation 3) can be explained if,

at longer times, the rate of reaction is limited by the availability of isolated reaction sites activated at temperature T . For PC-470 polycarbosilane, reaction sites are known to be single Si-H bonds and single Si-CH₃ bonds, which react with oxygen to form Si-OH in the temperature range of the present experiments [13, 22].

The higher initial rate of reaction must result from the availability of one or several alternate reaction path(s) for oxygen in polycarbosilane, for which potential reaction sites are much more rapidly exhausted. The similarity in thermal activation energies of k_1 and k_2 suggests some similarity in the nature of the initial reaction path(s) with that of the long-time reactions; however, the very high apparent value of n is unexplained.

By integration of Equation 5 with respect to time, the rate of heat generation, $Q_{\text{tot}} (d\alpha/dt)$, of polycarbosilane in air is then calculated

$$\frac{dQ}{dt} = Q_{\text{tot}} \left(k_1 \left\{ \frac{k_1}{(k_1 + k_2) \exp[k(n-1)t] - k_2} \right\}^{1/(n-1)} + k_2 \left\{ \frac{k_1}{(k_1 + k_2) \exp[k(n-1)t] - k_2} \right\}^{n/(n-1)} \right) \quad (9)$$

with Q_{tot} , k_1 , k_2 and n given by Equations 2, 6, 7 and 8, respectively. In summary, the set of Equations 2 and 6–9 describe empirically heat generation during the isothermal curing of polycarbosilane in air below 220 °C.

As a check of their precision, these equations were integrated numerically to predict curing exotherms under isothermal conditions over the temperature range 160–220 °C, and compared with the actual heat flow curves in Fig. 8a–d. As shown, the agreement is quite good (the slight mismatch seen in Fig. 8a stems from reaction not going to completion within the time-frame of the experiment). A comparison for the data taken at 140 °C is not presented, because the DSC signal was on the same scale as the system noise.

If we assume that the rate of curing is chiefly determined by the temperature and by the total number of bonds transformed, and neglect the possible influence of differences in the nature of transformed bonds with alterations in curing cycle, the empirical equations derived above can also be used to predict the heat released during non-isothermal curing cycles in air below 220 °C. Under this assumption, the rate of reaction, dQ/dt , is solely a function of temperature, T , and of the total heat given off by the reaction Q , which measures the number of available reaction sites. For any given curing cycle, then, the rate of reaction dQ/dt and the total heat given off, Q , can be calculated by integration of Equation 9, with T now a function of t .

The non-isothermal sequence of DSC runs (7 followed by 8), was performed to test the validity of this path-independence assumption. The heat generated by the curing reaction for run 7 is shown in Fig. 2a. This curve was integrated with respect to time, resulting in a curve for the cumulative heat of reaction, drawn with a dashed line in the figure. As seen, the heat liberated during run 7 was 1450 J g⁻¹. The heat

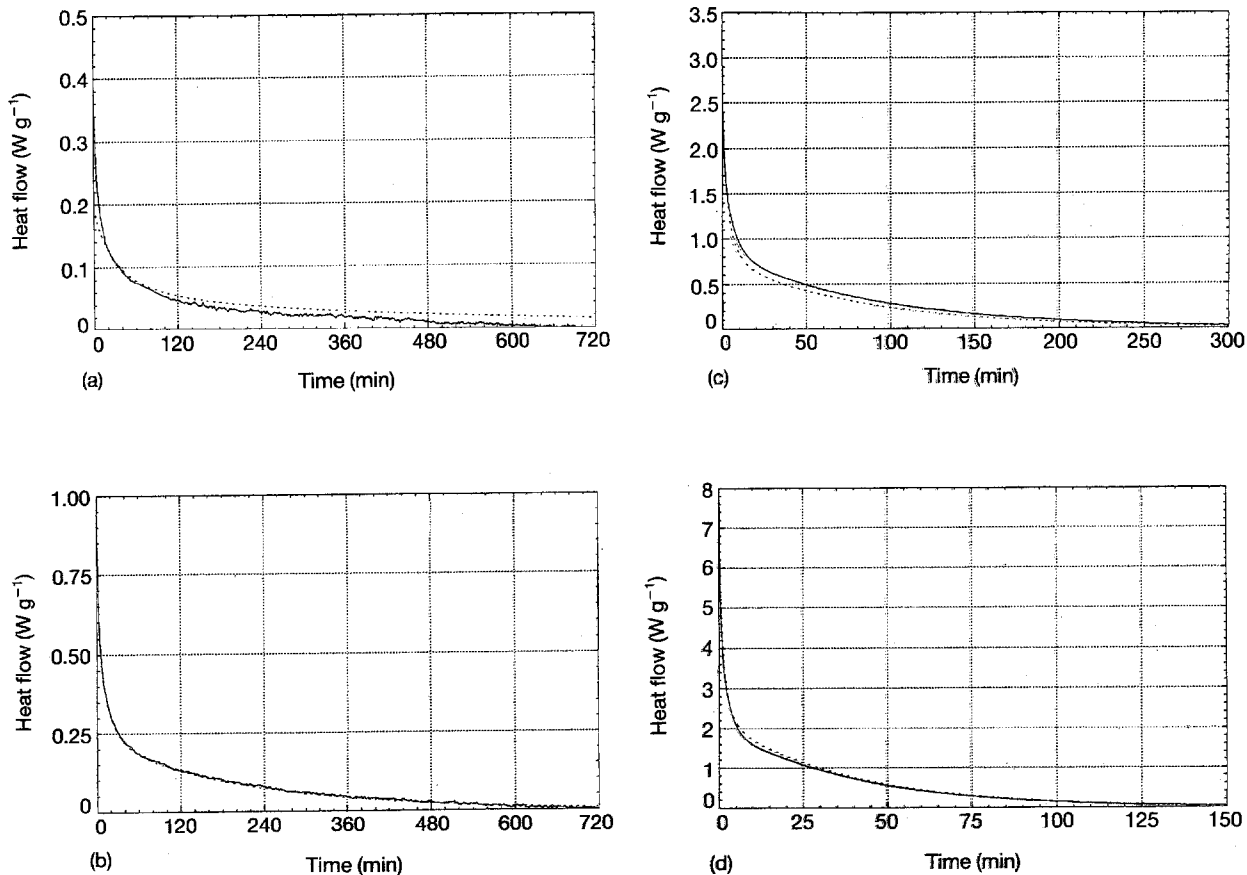


Figure 8 Comparison of heat flow (---) predicted by Equation 8 with (—) experimental data: DSC runs (a) 2, (b) 3, (c) 4, and (d) 6.

generated by the sample in run 8 is shown in Fig. 2b. This curve was integrated with respect to time, resulting in a curve for the cumulative heat of reaction, also drawn in the figure with a dashed line; the heat liberated during run 8 was 3720 J g⁻¹. The total heat of reaction generated during runs 7 and 8 sums to 5170 J g⁻¹, which agrees well with 5100 J g⁻¹ measured in the earlier isothermal run at 220 °C (run 6) on as-received PC.

The degree of conversion, α , after run 7 was calculated by dividing the heat liberated during run 7 by the sum of the heat liberated in runs 7 and 8. In doing so, the degree of conversion was found to be 0.280. The DSC curves from runs 7 and 8 were juxtaposed on to a single time axis as seen in Fig. 9. As seen, the heat flow rate at the beginning of the second run is slightly less than the heat flow rate at the end of the first run. This disparity is probably due to the reaction progressing to a slight extent during the cooling and heating cycles between the runs.

Fig. 10 shows the rate of heat generation versus time for both the as-received (run 6) and partially cured (run 8) polycarbosilane. In this figure the curve of

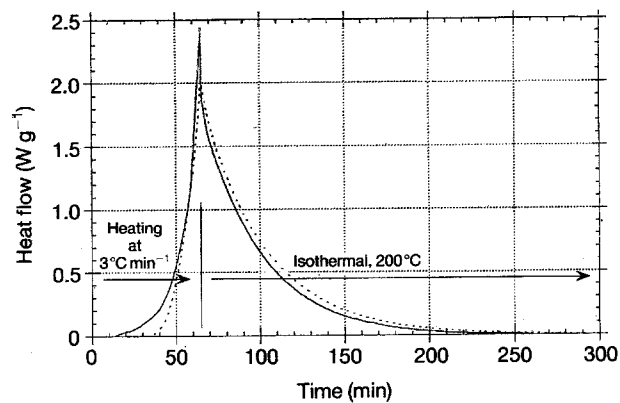


Figure 9 Cumulative heat flow rate for (—) non-isothermal runs 7 and 8 compared with (---) predictions of curing rate equations derived from isothermal experiments.

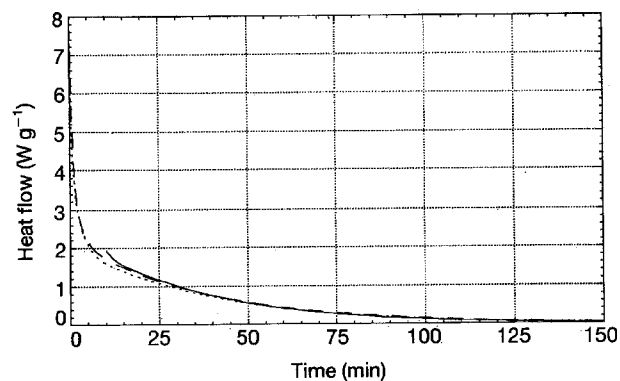


Figure 10 Curing exotherms of polycarbosilane in the as-received and partially cured states, in air at 220 °C, and compared with empirical equations. The curing isotherm of partially cured polycarbosilane is displaced horizontally to match the isothermal degree of conversion. (---) As-received (experimental); (---) As-received (simulated) and (—) Partially cured (experimental).

dQ/dt for run 8 has been shifted 9.9 min from the origin, to match the point in time where the sample in run 6 had a partial conversion of 0.280. As seen, the match between the curves is quite good, validating the assumption that the rate of generation is an exclusive function of T and Q . Experimental DSC curves for runs 7 and 8 are therefore compared in Fig. 9 with a simulated heat-flow curve based on Equations 2, and 5–8, generated by numerical integration for non-isothermal curing. Reasonable agreement exists between the experimental and simulated curves, demonstrating the validity of the equations for this non-isothermal heating path.

It is finally noted that Equation 5 of this work differs in form from that proposed by Suwardie and co-workers for commercial polycarbosilane [18, 19], Equation 1. Equation 1 predicts a maximum in the rate of curing at some non-zero time, which was not observed in the present investigation. Fig. 8 of [19] shows that the maximum is detected after several minutes at 200°C, which is longer than the minute spent heating the samples to the reaction temperature in the present experiments: the peak should have appeared in our experiments, particularly in DSC run 5, which was also performed at 200°C in oxygen. If our experimental data are correct, the maximum in the data of Suwardie and co-workers may have resulted from transient heat-transfer effects in the exchange of gases used in their procedure. We also note that the total heats of curing, Q_{tot} , measured by Suwardie and co-workers of 3612 cal g⁻¹, which corresponds to 15 100 J g⁻¹ (Table I of [19]), is much higher than what we found for the same experimental conditions with sample 5, namely 5300 J g⁻¹. Using data from Moore [23], we have estimated that the energy for full combustion of polycarbosilane is of the order of 41 kJ g⁻¹, while that for oxidative removal of all methyl side groups is 21 kJ g⁻¹; hence, both Suwardie and co-workers' and our data are plausible. We thus have no explanation to offer for the discrepancies between results of Suwardie and co-workers and our work, other than to state that if no error was made in experimental procedures, these must have arisen from differences in the nature of the commercial polycarbosilane used.

5. Conclusion

The total heat of curing of polycarbosilane in air below 220°C increases linearly with temperature. At a given temperature, the isothermal curing kinetics are well described by the sum of a first-order kinetic term, and a term of much higher order, near 10, both depending on the total fraction of remaining reaction enthalpy ($1 - \alpha$), as shown in Equation 5. Constants for both terms increase with temperature according to the Arrhenius law, with roughly the same activation energy.

If it is assumed that the rate of curing is solely a function of temperature and number of bonds transformed, measured by the heat of curing released, the equations can be used to predict the kinetics of curing of polycarbosilane in non-isothermal curing cycles below 220°C in air. Such path-independence of curing

kinetics was tested with a two-cycle non-isothermal curing experiment, for which good agreement was found between experiment, and predictions from equations resulting from isothermal experiments.

Acknowledgements

This work was sponsored by the Consortium for Inorganic Composites at MIT, and by a Kurtz Fellowship to T. Fitzgerald at MIT during the Fall of 1992. The authors thank Dr V. J. Michaud for several helpful discussions.

References

1. K. J. WYNNE and R. W. RICE, *Ann. Rev. Mater. Sci.* **14** (1984) 297.
2. W. H. ATWELL, in "Advances in Chemistry Series", edited by J. Zeigler and F. W. Gordon Fearon (American Chemical Society, Washington DC, 1990) pp. 593–606.
3. D. SEYFERTH, in "Advances in Silicon-Based Polymer Science", Conference Proceedings, Makaha, Oaha, HI, 1987, edited by J. M. Zeigler and F. W. Gordon Fearon (American Chemical Society, Washington, DC, 1990) pp. 565–91.
4. R. H. BANEY, J. H. GAUL and T. K. HILTY, in "Conference on Emergent Process Methods for High-Technology Ceramics", Materials Science Research Series Vol. 17, North Carolina State University, edited by R. F. Davis, H. Palmour III and R. L. Porter (Plenum Press, New York, 1982) pp. 253–62.
5. S. YAJIMA, in "Handbook of Composites", edited by W. Watt and B. V. Perov (Elsevier Science, Amsterdam, 1985) pp. 201–37.
6. K. K. CHAWLA, "Composite Materials, Science and Engineering" (Springer, New York, 1987) p. 292.
7. Y. HASEGAWA and K. OKAMURA, *J. Mater. Sci.* **18** (1983) 3633.
8. E. BOUILLON, F. LANGLAIS, R. PAILLER, R. NASSLAIN and F. CRUEGE, *ibid.* **26** (1991) 1333.
9. D. R. CLARKE, *J. Am. Ceram. Soc.* **75** (1992) 739.
10. Y. HASEGAWA, M. HIMURA and S. YAJIMA, *J. Mater. Sci.* **15** (1980) 720.
11. H. ICHIKAWA, F. MACHINO, S. MITSUNO, T. ISHIKAWA, K. OKAMURA and T. HASEGAWA, *ibid.* **21** (1986) 4352.
12. T. HASEGAWA, *ibid.* **24** (1989) 1177.
13. H. ICHIKAWA, F. MACHINO, H. TERANISHI and T. ISHIKAWA, in "Advances in Chemistry Series", edited by J. M. Zeigler and F. W. Gordon Fearon (American Chemical Society, Washington, DC, 1990) pp. 619–37.
14. T. TAKI, S. MAEDA, K. OKAMURA, M. SATO and T. MATSUZAWA, *J. Mater. Sci. Lett.* **6** (1987) 826.
15. T. TAKI, K. OHAMURA and M. SATO, *J. Mater. Sci.* **24** (1989) 1263.
16. T. TAKI, M. INUI, K. OKAMURA and M. SATO, *J. Mater. Sci. Lett.* **8** (1989) 918.
17. D. M. KALYON and S. KOVENKLIUGLU, *Adv. Polym. Technol.* **7** (1987) 191.
18. H. SUWARDIE, MSc thesis, Stephens Institute of Technology (1988).
19. H. SUWARDIE, D. M. KALYON and S. KOVENKLIUGLU, *J. Polym. Sci.* **42** (1991) 1087.
20. T. J. FITZGERALD, V. J. MICHAUD and A. MORTENSEN, *J. Mater. Sci.* **29** (1994) in press.
21. M. S. SPOTZ, PhD thesis, Massachusetts Institute of Technology (1990).
22. Y. HASEGAWA, *J. Mater. Sci.* **24** (1989) 1177.
23. W. J. MOORE, "Basic Physical Chemistry" (Prentice Hall, Englewood Cliffs, NJ, 1983).

Received 30 September 1993
and accepted 9 June 1994